HHS Public Access

Author manuscript

*Mol Cell Endocrinol*. Author manuscript; available in PMC 2024 February 06.

Published in final edited form as:

*Mol Cell Endocrinol*. 2023 August 01; 573: 111968. doi:10.1016/j.mce.2023.111968.

# Differential roles of insulin receptor in adipocyte progenitor cells in mice

**Yexian Yuan**[1,2,7], **Zuoxiao Shi**[2,3,7], **Shaolei Xiong**[2,7], **Ruoci Hu**[2,3], **Qing Song**[4], **Zhenyuan Song**[4], **Sang-Ging Ong**[5,6], **Yuwei Jiang**[2,3,8]

[1]Guangdong Laboratory of Lingnan Modern Agriculture, Guangdong Province Key Laboratory of Animal Nutritional Regulation and National Engineering Research Center for Breeding Swine Industry, College of Animal Science, South China Agricultural University, Guangzhou, 510642, China

[2]Department of Physiology and Biophysics, The University of Illinois at Chicago, Chicago, Illinois, 60612, USA

[3]Department of Pharmaceutical Sciences, The University of Illinois at Chicago, Chicago, Illinois, 60612, USA

[4]Department of Kinesiology and Nutrition, The University of Illinois at Chicago, Chicago, Illinois, 60612, USA

[5]Department of Pharmacology and Regenerative Medicine, College of Medicine, The University of Illinois at Chicago, Illinois, 60612, USA

[6]Division of Cardiology, Department of Medicine, The University of Illinois College of Medicine, Illinois, 60612, USA

[7]These authors contributed equally

## Abstract

The development of white adipose tissue (WAT) occurs during distinct embryonic and postnatal stages, and it is subsequently maintained throughout life. However, the specific mediators and mechanisms responsible for WAT development during different phases remain unclear. In this study, we investigate the role of the insulin receptor (IR) in regulating adipogenesis and adipocyte function within adipocyte progenitor cells (APCs) during WAT development and homeostasis. We use two *in vivo* adipose lineage tracking and deletion systems to delete IR either in embryonic APCs or adult APCs, respectively, to explore the specific requirements of IR during WAT development and WAT homeostasis in mice. Our data suggest that IR expression in APCs may not be essential for adult adipocyte differentiation but appears to be crucial for adipose tissue development. We reveal a surprising divergent role of IR in APCs during WAT development and homeostasis.

[8] Lead contact: Correspondence and requests for materials should be addressed to YJ (yuweij@uic.edu).

AUTHOR CONTRIBUTIONS

Y.J. conceived the project, designed the experiments, supervised the analyses, and edited the manuscript. C.S., R.H, O.S, Q.S, Y.Y, S.X and Z.S conducted most of the experiments and data analysis, wrote the first draft of the manuscript, and edited the subsequent versions. All the authors read and approved the manuscript.

The authors declare no conflict of interests.

**Keywords**

Insulin receptor; Adipocyte progenitor cells; Adipose tissue development; Tissue homeostasis; Lipodystrophy

## INTRODUCTION

White adipocytes are critical for storing excess nutrients and circulating fatty acids as triglycerides. These stored triglycerides can then be mobilized and used in response to metabolic demands to fuel target tissues. In addition to lipid storage, white adipocytes serve as active endocrine cells that control many metabolic responses such as inflammation, glucose homeostasis, and insulin sensitivity. Hence, proper white adipocyte function is essential for metabolic flexibility and health (Kershaw and Flier, 2004; Rosen and Spiegelman, 2006; 2014; Spiegelman and Flier, 2001; Trayhurn and Beattie, 2001). However, in response to uncontrolled pathophysiological expansion of white adipose tissue (WAT), a core attribute to obesity, white adipocyte lipid storage and endocrine function become dysregulated, leading to metabolic disorders, including insulin resistance, chronic inflammation, fibrosis, and atherosclerosis (Coutinho et al., 2011; Emerging Risk Factors et al., 2011; Phillips and Prins, 2008; Pischon et al., 2008; Sun et al., 2011). Yet, despite the importance of white adipocytes in regulating various local and systemic metabolism, our understanding of the factors and mechanisms controlling adipocyte development and homeostasis, *in vivo*, remains poorly defined.

Recent studies have identified that adipocytes can arise from two distinct phases: a developmental phase and an adult phase (Jiang et al., 2014; Knittle et al., 1979; Shin et al., 2020b; Spalding et al., 2008; Tang et al., 2008; Wang et al., 2013). In rodents, the developmental phase consists of embryonic specification and patterning of adipocyte progenitor cells (APCs) and their postnatal lipid filling. The adult phase or homeostatic phase is the utilization of APCs to generate new adipocytes throughout the organism's lifespan in response to various environmental cues, such as nutritional status and temperature. This homeostatic phase replenishes the tissue with new adipocytes, allowing turnover of existing adipocytes to maintain metabolic health. Recent studies have focused on understanding adult APC identity and their ability to generate new adipocytes. Specifically, adult APCs reside within the adipose tissue vascular niche and appear to resemble a specialized subset of mural cells (smooth muscle cells, pericytes) (Jiang et al., 2014; Tang et al., 2008; Traktuev et al., 2008; Vishvanath et al., 2016). They express mural cell markers such as smooth muscle actin (Sma), and platelet derived growth factor receptor β (Pdgfrβ). Adult APCs can be further identified based on their expression of the major transcriptional regulator of adipocyte differentiation, peroxisome proliferator activated receptor gamma (Pparγ) (Berry et al., 2016a; Jiang et al., 2017b; Shin et al., 2020a; Tang et al., 2008). Fate mapping studies, using Sma-genetic models, have demonstrated that Sma+ adult perivascular APCs can generate new adipocytes under normal homeostatic (or chow-fed) conditions at appreciable rates (Jiang et al., 2014). Moreover, modulating Pparγ expression, either up or down, within Sma+ cells can influence whether new adipocytes are formed

(Jiang et al., 2017b; Jiang et al., 2014). However, the full spectrum of *in vivo* adipogenic mediators has yet to be defined within the APC population.

Insulin receptor (IR) signaling has been regarded, both *in vitro* and *in vivo*, as a key component in controlling glucose homeostasis and lipid storage (Boucher et al., 2014; Czech, 2017). In agreement with this notion, studies using tissue-specific knockouts of IR, have defined its role in glucose sensing and lipid accumulation in several tissues, including muscle, liver, pancreatic beta-cells, brain, and adipose tissue (Bluher et al., 2003; Bluher et al., 2002; Bruning et al., 2000; Bruning et al., 1998; Joshi et al., 1996; Katic et al., 2007; Kitamura et al., 2003; Kulkarni et al., 1999; Mauer et al., 2010; Pratipanawatr et al., 2001; Qiang et al., 2016; Sakaguchi et al., 2017). In adipose tissue, deleting IR in mature adipocytes using aP2-Cre, a quasi-fat specific Cre driver, reduced fat content with regular insulin and glucose sensitivity (Bluher et al., 2002). Using a more restricted adipose tissue-specific (Adiponectin-Cre) Cre line to delete IR resulted in lipodystrophy and metabolic dysfunction (Qiang et al., 2016). Using an inducible mature adipocyte driver adiponectin-$Cre^{ERT2}$ to delete IR, Kahn and colleagues recently demonstrated that loss of IR in mature adipocytes resulted in the rapid loss (3 days post tamoxifen) of fat cells and ensuing metabolic dysfunction (glucose and insulin intolerance and liver steatosis). Interestingly, this rapid loss of adipocytes stimulated adipocyte progenitors to proliferate and regenerate WAT, restoring metabolic function (Sakaguchi et al., 2017). However, the specific role of IR in APCs *per se* and its contribution to WAT development or adult WAT homeostasis have not been fully explored.

In this study, we examined whether IR is a mediator of WAT organogenesis or adult homeostasis. Towards this end, we employed two *in vivo* adipose lineage tracking and deletion systems to explore the specific requirements of IR function in the adipogenic cascade. Our results show that adult Sma+ APCs do not require IR for the formation of adult white adipocytes or cold-induced beige adipocytes derived from a Sma+ source. Instead, IR expression in developmental Ppar$\gamma$+ APCs appears to be necessary for WAT development. Furthermore, embryonic APC IR expression is required for WAT development, lineage expansion, and lipid biogenesis. Our findings reveal a surprising role for IR in APC function, acting as a critical regulator for adipose tissue specification and lipid accumulation during WAT development, yet it appears to be less essential for maintaining WAT homeostasis in adults.

## RESULTS

### Deleting IR within Ppar$\gamma$+ APCs promotes lipodystrophy

To examine the role of IR within the adipose lineage, we first assessed if IR was enriched in APCs by employing the AdipoTrak (AT) adipose specific lineage tracking system (Tang et al., 2008). AdipoTrak incorporates a tetracycline transactivator (tTA) allele knocked into the endogenous locus of the Ppar$\gamma$ gene, thus providing adipose lineage restriction. The Ppar$\gamma$-tTA allele has been combined with the Tet-responsive nucleotide labeling system, TRE-H2B-GFP, to identify proliferating and committed APCs within the stromal vascular (SV) compartment (Tang et al., 2008). Of note, AT marked APCs have been shown to be highly adipogenic and are necessary and sufficient for both WAT organogenesis and adult

WAT homeostasis (Jiang et al., 2014). We isolated floated lipid laden adipocytes and FACS isolated AT-GFP positive and negative SV cells and examined them for IR gene expression. We found that IR mRNA expression was enriched within AT-GFP+ APCs and adipocytes compared to other WAT SV cells (Figure 1A), suggesting that IR may have a functional role in APC biology. To examine the relevant role(s) of IR in APCs, we integrated an $IR^{fl/fl}$ allele with the AT tracking (*PPAR*$\gamma^{tTA}$*; TRE-H2B-GFP*) and deletion (*TRE-Cre*) mouse model termed (AT-IRKO) (Figure 1B). As expected, IR mRNA levels were significantly reduced from both subcutaneous inguinal WAT (iWAT) and visceral perigonadal WAT (gWAT) compartments compared to control AT-GFP+ cells (Figure 1C). We next examined 2-month-old AT-IRKO mice for possible adipose phenotypes; sibling controls contained the Ppar$\gamma$-tTA allele as well as either TRE-Cre or $IR^{fl/fl}$ alleles. Nuclear magnetic resonance (NMR) analysis of the fat content in AT-IRKO mice revealed a redistribution of body composition without significant changes in total body weight (Figure 1D). There was a 60–70% reduction in total body fat, accompanied by an increase in lean body mass (Figure 1E and Supplementary Figure 1A). Consistently, WAT depot sizes from AT-IRKO mice were considerably smaller than AT-Control WAT depots (Figure 1F–G). Our analysis showed no significant difference in food intake between the AT-IRKO and AT-Control groups (Supplementary Figure 1B). Histologically, hematoxylin and eosin (H&E) staining revealed the lack of adipocytes within the iWAT sections from AT-IRKO compared to AT-Control iWAT (Figure 1H). A similar trend was shown in gWAT, with few remaining adipocytes engorged in AT-IRKO gWAT (Supplementary Figure 1E). Trichrome collagen staining of AT-IRKO iWAT sections showed an increase in fibrotic tissue replacement compared to control iWAT (Figure 1I). Accordingly, mRNA expression analysis revealed the lack of adipocyte marker genes but an increase in fibroblast markers in AT-IRKO iWAT depots (Supplementary Figure 1F). Classical brown adipose tissue (BAT) was also significantly disrupted with a reduced number of brown adipocytes and lower mRNA expressions of BAT markers (Supplementary Figure 1G–H).

Lipodystrophy is characterized by the pathological loss of adipose tissue, which is often accompanied by various metabolic disorders, such as hyperlipidemia, hypercholesterolemia, ectopic lipid deposition, and insulin resistance. As AT-IRKO mice displayed a lipodystrophic phenotype, we hypothesized that they might also have other metabolic disturbances. Consistent with this, serum levels of blood cholesterol and triglycerides were elevated in AT-IRKO mice compared to the control group (Supplementary Figure 1C). Additionally, AT-IRKO mice showed hepatomegaly accompanied by hepatic steatosis (Supplementary Figure 1D and 1I). To evaluate insulin resistance and glucose handling, we conducted fasting, glucose, and insulin tolerance tests on both AT-Control and AT-IRKO mice. In line with lipodystrophy and impaired glucose responses, fed glucose levels were higher in AT-IRKO mice, although their fasting blood glucose clearance rate was comparable to that of the control group (Figure 1J). Yet, surprisingly, glucose and insulin tolerance tests indicated no significant difference between the mutants and controls (Figure 1K–L). Taken together, these results suggest that deleting IR in the adipose lineage disrupts the formation of white adipose tissue and causes metabolic imbalance, but insulin responses remain preserved.

### HFD does not restore fat formation in IR mutant mice

APCs can be provoked by exercise, thiazolidinediones (TZDs) and high-fat diet (HFD) to proliferate and differentiate into mature adipocytes (Tang et al., 2011; Zeve et al., 2016). We therefore examined if treating AT-IRKO mice with HFD could incite APCs to generate new adipocytes. Of note, this test was not to evaluate the deleterious effects of HFD on lipodystrophic mice but rather the ability to mobilize IR-deficient APCs into generating new adipocytes. Two-month-old AT-Control and AT-IRKO mice were fed a HFD for 12 weeks, and their phenotypes were evaluated (Supplementary Figure 2A). Throughout the HFD duration, AT-IRKO mice had similar body weight to the control group (Figure 2A). Importantly, AT-IRKO remained fatless (Figure 2B). Both AT-IRKO subcutaneous (iWAT and psWAT) and visceral adipose depots (gWAT, rWAT, mWAT) were significantly reduced compared to HFD fed controls (Figure 2C–D). Histologically, AT-IRKO iWAT was largely devoid of adipocytes, while gWAT adipocytes appeared hypertrophied (Figure 2E). Additionally, the reduced adiposity in HFD AT-IRKO mice was associated with decreased expression of adipocyte gene markers (Figure 2F). Unlike with a normal chow diet, HFD feeding worsened insulin responses in AT-IRKO mice compared to HFD-fed control mice (Figure 2G and Supplementary Figure 2B). Furthermore, AT-IRKO mice showed increased liver steatosis compared to the control group (Supplementary Figure 2C). Collectively, these data suggests that IR is critical for establishing adipose tissues and the impairment of adiposity caused by IR deletion in APCs cannot be restored by HFD treatment.

### IR loss in adult Sma+ APCs does not impair white adipogenesis derived from Sma+ sources.

Because the AdipoTrak lineage tracking and deletion system marks the entire adipose lineage (stem to adipocytes), we next evaluated if IR contributes to adult APC WAT homeostasis by combining the $IR^{fl/fl}$ mouse model with the mural cell inducible Cre driver, Sma-$Cre^{ERT2}$ (Sma-IRKO) (Figure 3A). The Sma-$Cre^{ERT2}$ model, when combined with the indelible rosa26-flox-stop-flox-tdTomato ($R26R^{RFP}$) fate mapping system, has been shown to label a subset of the adult APC compartment that can generate new adipocytes under adult WAT homeostatic conditions (Jiang et al., 2014). We administered one dose of tamoxifen (TMX) for two consecutive days and mice were analyzed six-weeks later (Figure 3A). Directed qPCR analysis confirmed reduced IR mRNA expression within the Sma compartment (Supplementary Figure 3A). We found that deleting IR within the Sma APC compartment did not impact body weight or glucose and insulin responses (Figure 3B–D). In agreement, fat content and adipose tissue weight were similar between SMA-Control and Sma-IRKO mutant mice (Figure 3E–G). Histologically, adipocyte size and architecture were conserved between control and mutant iWAT and gWAT specimens (Figure 3H). Consistently, mRNA expression levels of mature adipocyte markers were equivalently expressed between control and mutant iWAT samples (Figure 3I). In addition, we did not observe lipodystrophic metabolic disorders such as liver steatosis in Sma-IRKO mice, as detected in the AT-IRKO mice (Supplementary Figure 3B).

We next examined if new adipocytes were generated from Sma+ APCs lacking IR by performing fate mapping analysis of iWAT and gWAT sections from controls (Sma-RFP) and mutants (Sma-IRKO-RFP). By whole-mount immunofluorescent imaging, we found

that Sma+ cells could make adipocytes in both control and mutant iWAT (Figure 4A). In agreement, immunostaining revealed the presence of newly generated RFP+ adipocytes within iWAT from both control and mutant mice (Figure 4B). Quantification of RFP+ adipocytes confirmed that Sma+ cells deficient in IR were able to make a similar number of new adipocytes as controls (Figure 4C). Further, these newly generated adipocytes were similar in diameter (Figure 4D). Next, we examined if deleting IR influenced APC proliferation by administering 5-bromo-2'-deoxyuridine (BrdU; 10 mg/Kg for 24 hours) to both TMX induced Sma-control- and Sma-IRKO-RFP mice. RFP+ cells were FACS isolated from control and mutant iWAT depots and stained for BrdU. Flow cytometric analysis revealed that both control and mutant mice had a similar number of Sma-RFP+ cells and had a similar rate of BrdU incorporation (Figure 4E–F). We next tested their adipogenic capacity *in vitro* by isolating SV cells from 4-month-old TMX pulsed control and mutant mice. We found that both control and mutant SV cells had similar adipogenic capacity as assessed by Oil Red O, triglyceride accumulation, and adipocyte marker expression (Figure 4G–I). Together these data suggest that IR expression in adult Sma+ APCs may not be essential for the white adipogenesis process derived from Sma+ sources.

## IR loss in adult Sma+ APCs does not impair cold-induced beige adipogenesis derived from Sma+ sources.

The results indicate that IR expression in APCs is not necessary for adult white adipocyte formation. However, Sma+ APCs have been shown to give rise to cold temperature-induced beige adipocytes in adults (Berry et al., 2016b; Jiang et al., 2017a). To determine whether IR-deficient Sma+ cells can form beige adipocytes in response to cold temperatures, we treated Sma-Control and Sma-IRKO mice with a single dose of TMX for two consecutive days and allowed for a two-week TMX washout period before exposing the mice to cold temperatures (6°C) (Figure 5A). Throughout cold exposure, body temperature defense, which serves as a surrogate for beige fat formation, appeared comparable between control and mutant mice (Figure 5B). Although food intake and serum triglycerides were similar between the two groups, we observed an increase in serum glucose levels and a decrease in serum free fatty acids (Figure 5C–F). However, Sma-Control and Sma-IRKO mice showed similar adipose tissue weights, beige adipocyte histological appearance, beige and thermogenic gene expression, as well as uncoupling protein-1 (Ucp1) immunohistochemistry (IHC) (Figure 5G–J and Supplementary Figure 4A–B). In addition, we isolated SV cells from control and mutant mice and cultured them in beige adipogenic media, which revealed comparable beiging potential based on Oil Red O staining (Supplementary Figure 4C). Overall, our findings indicate that the expression of IR in SMA+ APCs is not essential for the development of white or beige adipocytes derived from Sma+ sources during adulthood.

## IR expression in Ppar$\gamma$+ APCs is required for WAT organogenesis

Our data suggest that IR has a limited role in regulating adult Sma-APC adipogenic potential. Therefore, the lipodystrophic phenotype observed in AT-IRKO mice may result from a WAT developmental phenotype. To investigate this, we re-examined AT-IRKO mice and analyzed mice at postnatal day 10 (P10) (Figure 6A), a developmental stage when all subcutaneous adipose depots are filled with lipids. We found that AT-IRKO

mice exhibited decreased body weight and significantly reduced subcutaneous iWAT (Figure 6B–C). Histological examination of AT-IRKO iWAT and psWAT depots showed a substantial absence of adipocytes (Figure 6D), which was supported by a lack of perilipin-1 immunostaining. However, AdipoTrak-labeled GFP+ APCs were correctly located in iWAT sites, as shown by whole-mount GFP imaging and histological analysis (Figure 6E–F).

The above data suggest that IR plays a critical role in adipose tissue development, and its inactivation may disrupt APC lineage dynamics and prevent adipocyte lipid filling. To investigate whether IR inactivation affects adipocyte progenitor lineage decisions, we used the TRE-H2B-GFP reporter to label the progenitors in AT-IRKO mice. GFP expression indicates continued Pparγ expression in the APC lineage, while reduced GFP expression may suggest reduced progenitor numbers or dampened Pparγ expression. Using flow cytometry, we analyzed the total GFP cellular numbers in iWAT and evolving gWAT depots from P10 AT-Control and AT-IRKO mice. We observed that AT-IRKO WAT depots had decreased AT-GFP cell numbers (by 75% in iWAT and 30% in gWAT) compared to P10 controls (Figure 7A). We also examined E16.5 embryos for AT-GFP+ anatomical patterning and found that AT-IRKO-GFP+ cells were present in the correct anatomical anlage but showed reduced GFP intensity (Figure 7B). To investigate whether IR inactivation altered the fate of adipocyte progenitors, we introduced a R26RRFP allele into AT-IRKO mice to permanently label APCs and their descendants. Flow cytometry analysis showed a decrease in RFP numbers in both iWAT and gWAT P10 depots (Figure 7C), suggesting that IR inactivation did not induce changes in the adipose lineage but possibly reduced APC proliferation rates. Flow cytometry analysis also revealed that P10 AT-IRKO mice had reduced BrdU incorporation into GFP+ APCs after a 24-hour BrdU pulse (Figure 7D). These findings were further supported by monitoring BrdU incorporation *in vitro* of FACS-isolated AT-GFP+ cells from control and mutant mice (Figure 7E).

We also evaluated the adipogenic potential of SV cells isolated from control and AT-IRKO mutant mice. Our results showed that the AT-IRKO mutant SV cells were unable to differentiate into mature adipocytes, as evidenced by their lack of Oil Red O staining, reduced triglyceride accumulation, and decreased expression of adipocyte markers (Figure 7F–H). Together, these data suggest that APC expression of IR is required for WAT organogenesis by regulating the proliferation and differentiation of stem/progenitor cells.

## IR in Pparγ+ APCs regulates genes involved in lipid biosynthesis and APC “stemness”

To further explore potential molecular mechanisms, we FACS isolated control AT-GFP+ and AT-IRKO-GFP+ cells and examined the downstream signaling and transcriptional events. We first examined the phosphorylation status of AKT, the main positive effector of glucose uptake and lipogenesis, and downstream target of IR signaling (Taniguchi et al., 2006). We found that AT-IRKO GFP+ APCs, within iWAT and evolving gWAT, had a reduction in AKT phosphorylation at site Ser473 (Figure 7I). Correspondingly, we also observed a significant reduction in common lipogenic genes, including fatty acid synthase, CD36 (a fatty acid transporter), and perilipin-1, in the AT-IRKO GFP+ cells (Figure 7J). Since AT-IRKO had reduced APC proliferation and lineage expansion, we further examined expression levels of the key “stemness” genes in control AT-GFP+ and AT-IRKO-GFP+ cells. We found that

Pparγ and Zfp423 were reduced in AT-IRKO-GFP+ cells (Figure 7K). Thus, it appears that IR is critical for WAT development, and APC lineage expansion and lipid biogenesis via controlling downstream transcriptional events, potentially mediated by AKT signaling.

## DISCUSSION

APC function impacts adipose tissue development and maintenance. Recent studies have shown that developing APCs are distinct from adult APCs, highlighted in part by their distinct micro-anatomical, functional, and molecular profiles. Insulin signaling has long been recognized as an important regulator of adipogenesis and adipocyte function. Thus, given the therapeutic potential of targeting the insulin pathway to improve adipose tissue health and to mitigate metabolic disease, it is imperative to understand if IR regulates WAT organogenesis and/or WAT homeostasis. Here, we report that adult APC dynamics and adipocyte formation are not critically dependent on IR. However, deleting IR specifically within developing APCs resulted in diminished progenitor kinetics, including reduced proliferative and adipogenic potential, while still being able to localize to the correct anatomical anlagen. Mechanistically, we found that IR regulates expression of adipogenic and lipid biogenic genes to control lipid filling, as well as proliferative potential, potentially through phosphorylated AKT levels. Our findings suggest that IR is differentially required for adipogenesis at different stages of life, highlighting distinct regulatory mechanisms governing WAT development versus WAT homeostasis *in vivo*.

Recent efforts have begun to establish the presence of distinct regulatory mechanisms governing WAT development versus WAT homeostasis. For example, Akt2 is not necessary for WAT development but is required for CD24+ adipose progenitor cell proliferation in postnatal animals (Jeffery et al., 2015), while C/ebpα is critical for WAT expansion during HFD or in Leptin-deficient mice but not necessary for WAT maturation and maintenance during fetal and early postnatal development (Wang et al., 2015). Additionally, a recent study from Gupta and colleagues suggests that fetal function of Zfp423 is distinct from Zfp423 in adult WAT (Shao et al., 2017). This concept may also be critical for perivascular cold-induced beige adipocyte formation (Angueira et al., 2021). Thus, multiple lines of evidence support that developing and mature WATs have unique progenitor pools that utilize distinct regulatory mechanisms to respond to developmental and nutritional cues. Evidence suggests that embryonic development is crucial for establishing WAT mass and the number of adipocytes, which remains relatively constant in adulthood, with approximately 10% of adipocytes turning over in humans each year (Spalding et al., 2008). It is plausible that adult APCs have low proliferative capacity to maintain WAT homeostasis, while developing APCs are designed to be proliferative for organ expansion and establishment. Our data demonstrate that IR is critical for the initial establishment of WAT by controlling the number of APCs and their lipid accumulation ability. It is also possible that the reduced number of GFP-positive APCs in AT-IRKO mice is attributed to increased apoptosis of APCs, consequently affecting the overall APC population in the WAT of AT-IRKO mice. However, IR seems to be dispensable in adult Sma+ APCs. The major differences between developing and adult APCs remain largely unknown, and future studies that identify these distinct progenitor pools genetically and phenotypically would provide further insights into WAT development and maintenance.

Recent evidence has demonstrated that the regulation of WAT in adult animals is more complex than previously thought. Studies, including our own, have shown that adipose progenitors proliferate and generate new adipocytes in response to external stimuli such as HFD, exercise, and TZDs during adipose tissue remodeling (Tang et al., 2011; Vishvanath et al., 2016; Wang et al., 2013; Zeve et al., 2016). Moreover, de novo adipogenesis has been observed during regeneration of adult WAT after ablation, as well as in muscle tissue adipogenesis following injury, wound healing, bone marrow transplantation, and irradiation, in addition to white adipogenesis during normal development and obesogenic expansion (Horsley and Watt, 2017; Majka et al., 2010; Plikus et al., 2017; Reyne et al., 1983).
It appears that the formation of adipocytes in WAT homeostasis and other adipogenesis conditions may arise from different cellular sources and be controlled by distinct molecular mechanisms. By using the Sma+ mural cell lineage tracking system, we have provided direct genetic evidence demonstrating that Sma+ cells play a crucial role in maintaining WAT under normal homeostasis (Jiang et al., 2014). However, it is still unclear whether Sma+ mural cells also contribute to adipogenesis under other conditions, such as a high-fat diet. For instance, lineage tracing studies from Dr. Gupta's group using a Pdgfrβ doxycycline-inducible mural tracking system (Pdgfrβ-rtTA) revealed that Pdgfrβ+ cells give rise to adipocytes associated with diet-induced obesity but not under normal tissue homeostasis (Vishvanath et al., 2016). A more recent study from the same group has used a Pdgfrβ-rtTA mice to overexpress *Pparg* in PDGFRβ+ APCs, which improved their adult stage adipose tissue plasticity to resist HFD induced obesity and diabetes (Zhang et al., 2022). Our data appear to suggest that the adipogenesis process in adult Sma+ APCs may not be critically dependent on IR expression. Yet, if IR controls adipogenesis under HFD in adult animals, it will be an important future avenue of study.

Recent studies have also suggested that vascular smooth muscle progenitors, including Sma+ cells, can generate beige adipocytes in response to cold stimulation (Berry et al., 2016b; Long et al., 2014; Shamsi et al., 2021). Towards this end, we analyzed the role of IR in beige adipogenesis originating from Sma+ APCs. Our findings suggest that IR is not necessary for de novo beige adipogenesis from Sma+ progenitors after one week of cold exposure. However, other lineage tracing studies have proposed that multiple waves of beige adipogenesis may occur. For example, Myh11+ cells and Pdgfrβ+ cells were found to give rise to some beige adipocytes after 2 weeks of cold challenges (Long et al., 2014; Vishvanath et al., 2016). Our recent research also indicates that beta3-induced beige adipocytes come from different cellular sources than those generated by cold-induced beige adipocytes (Jiang et al., 2017a). Therefore, it would be intriguing to investigate whether IR plays a role in beige adipogenesis under these circumstances.

Although we have extensively examined the role of APC expression of IR in adult mouse adipogenesis, one question that still remains is whether different functions of IR can affect other crucial steps in adult tissue homeostasis. For example, we have previously shown that adult APCs appear to be specified at embryonic day 10.5 (E10.5) and function later in adult WAT homeostasis (Tang et al., 2008). These E10.5 cells appear to arrive at WAT depots, once WAT organogenesis is completed (~P30), to regulate adult WAT homeostasis and metabolism. Functional manipulation of IR specifically in these cells and then following their fate and location will help clarify the importance of IR in APC niche-homing and

niche expansion. Previous research has demonstrated that IR plays important roles in mature adipocytes. Dr. Ronald Kahn's group has used an Adiponectin-Cre mouse line to knock-out IR in mature adipocytes, where 3-month-old Adiponectin-Cre IR knockout mice showed severe metabolic dysfunction phenotypes including both insulin resistance and glucose tolerance (Boucher et al., 2016). However, our Sma-IR model has revealed that mutant adipocytes without IR appear to function normally. One possible explanation for this is the proportion of mutant adipocytes in relation to the wild-type adipocyte population. For example, our lineage tracing data suggest that 10–20% of new adipocytes generated from Sma+ sources per month, meaning that 80–90% of adipocytes would still be considered wild-type for IR and function normally. This hypothesis could be tested using genetic methods to continuously eliminate IR function in the progenitor pool. Several studies have proposed that insulin-like growth factor 1 receptor (IGF-1R) and IR have overlapping roles in multiple tissues (Belfiore et al., 2009; Nakae et al., 2001). Thus, it remains to be examined if IGF-1R becomes hyperactive in adult IR-deficient APCs as an attempt to compensate for the absence of IR.

In summary, our study expands current knowledge concerning IR function in APCs during WAT development and maintenance. By utilizing several genetic tools to delete IR in APCs in a spatiotemporal-controlled manner, we find that APC expression of IR is essential for APC proliferation and differentiation during WAT organogenesis. However, IR may not be necessary for adipogenesis in the adult stage from SMA+ APCs. These data highlight the emerging notion that different regulatory mechanisms govern the developmental and adult WAT and may help shed insight into the new therapeutic targets for treatment or prevention of childhood and adult obesity and their associated metabolic co-morbidities.

## MATERIALS AND METHODS

### Animals

Mice were maintained under the guidelines of the UT Southwestern Medical Center Animal Care (UTSW) or the Biological Resource Laboratory, University of Illinois at Chicago (UIC). All animal experiments and procedures were approved by the Institutional Animal Care and Use Committees at UTSW and UIC. Mice were housed in a 12:12 light:dark cycle and chow and water were provided ad libitum. AdipoTrak mice are defined as PPAR$\gamma$-tTA; TRE-Cre; TRE-H2B-GFP as previously established in our lab (Tang et al., 2008). PPAR$\gamma$-tTA (stock No: 024755), $IR^{fl/fl}$ (stock no: 006955) and $R26R^{RFP}$ (stock no: 007908) mice were obtained from the Jackson Laboratory. SMA-$Cre^{ERT2}$ mice were generously provided by Dr. Pierre Chambon. Cre recombination was induced by administering one dose of tamoxifen dissolved in sunflower oil (Sigma, 50 mg/Kg intraperitoneal injection) for two consecutive days. In these experiments, tamoxifen was given to all animal groups including control mice, which carried the floxed alleles but lacked the Cre transgene or carried the Cre but lacked floxed alleles. The mice were fed either normal chow (4% fat, Harlan-Teklad, Madison, WI) or HFD (60%, D12492, Research diets). BrdU (Sigma, 19–160) was IP injected (100 mg $kg^{-1}$ body mass) or provided in the drinking water (0.5 mg $ml^{-1}$ in 1% sucrose).

### Stromal Vascular Fractionation Isolation

Stromal-vascular (SV) cells were isolated as previously described (Tang et al., 2008). Subcutaneous (inguinal, interscapular) white adipose tissues were pooled for fractionation, unless indicated otherwise. After 2 hours of slow shaking in isolation buffer (100mM HEPES pH7.4, 120mM NaCl, 50mM KCl, 5mM glucose, 1mM CaCl2, 1.5% BSA) containing 1mg/ml collagenase type 1 (Worthington Biochemical, CLS-1) at 37°C, the suspension was then spun at 800g for 10 minutes and the pellet contained a crude SV fraction. The floating adipocyte layer was washed in 1X PBS, spun at 800g for 5 minutes, and the solution was removed from below. The SV pellet was then resuspended in erythrocyte lysis buffer (155 mM $NH_4Cl$ in $H_2O$) for 5 minutes, spun at 800g for 5 minutes. The pellet was washed once in 1X PBS, resuspended and passed through 40μm mesh. The pellet was then resuspended in growth media (DMEM (Corning, 10013CV) supplemented with 10% FBS (Sigma-Aldrich, F6178), 1% Penicillin-streptomycin (Gibco, 15140122), and 0.1% Amphotericin B (Sigma-Aldrich, A4888).

### Cell Culture

Isolated mouse SV cells were cultured in DMEM supplemented with 10% FBS. White adipogenesis was induced by treating confluent cells with DMEM containing 10% FBS, insulin (1 μg/ml, Sigma-Aldrich, I0516), dexamethasone (5 μM, Cayman Chemicals, 11015), and isobutylmethylxanthine (0.5 mM, Sigma-Aldrich, I5879) for 3 days. Beige adipogenesis was induced by treating confluent cells with DMEM containing 10% FBS, insulin (1 μg/ml, Sigma-Aldrich, I0516), dexamethasone (5 μM, Cayman Chemicals, 11015), isobutylmethylxanthine (0.5 mM, Sigma-Aldrich, I5879), rosiglitazone (1 μM, Cayman Chemicals, 71740), and T3 (2 nM, Cayman Chemicals, 16028). To induce beige and thermogenic genes, cells were treated with 10 μM forskolin (Sigma-Aldrich, F3917) for 4 hours and harvested to collect mRNA (Wu et al., 2012). Triglyceride accumulation was performed using a kit from ZenBio (TG-1-NC) (Berry and Noy, 2009; Berry et al., 2010) and manufacturer's protocol was followed.

### Flow Cytometry

SV cells were isolated and washed, centrifuged at 800g for 5min, and analyzed with a FACS analyzer or sorted with a BD FACS Aria operated by the UT Southwestern Flow Cytometry Core. Data analysis was performed using BD FACS Diva software. For GFP+ and RFP+ sorting, live SV cells from *PPARγ$^{tTA}$; TRE-Cre; TRE-H2B-GFP*; *R26R$^{RFP}$* control and IR deletion were stained with propidium iodide (PI, 1mg/ml) to exclude dead cells and sorted based on native fluorescence (GFP and RFP). The SV cells from GFP− and RFP− mice were used to determine background fluorescence levels. The dissociated SV cells were also analyzed for BrdU (rat-anti-BrdU, 1:100, Abcam, ab6326) and pAKT (anti-pSer473-AKT, 1:100, Cell signaling, 9271) by flow cytometry. Briefly, SV cells were incubated with primary antibodies on ice for 30 minutes. Cells were then washed twice with staining buffer and incubated with secondary antibodies for another 30 minutes on ice before being analyzed by flow cytometry.

## Quantitative real-time PCR (qPCR)

Total RNA was extracted from mouse tissues or cells using TRIzol (Invitrogen). High-capacity RNA to cDNA kit (Life technologies) was used for cDNA synthesis. Power SYBR Green PCR Master Mix with ABI 7500 Real-Time PCR System was used for gene expression analysis. qPCR values were normalized to 18s rRNA expression. Subcutaneous inguinal adipose depots were used for measuring mRNA levels of beige and thermogenic genes, unless otherwise specified.

## Histological Staining

Hematoxylin and eosin (H&E) or Trichrome staining was carried out on paraffin sections using standard methods (Tang et al., 2008; Zeve et al., 2012). Adipose tissues were fixed in formalin overnight. Tissues were then processed in STP120 tissue processing unit (Thermo-Fisher Scientific, 813160) in a series of alcohol dehydrated steps and xylene rinses. Tissues were then embedded in paraffin using a HistoStar™ tissue embedding station (Thermo-Fisher Scientific, A81000001). Embedded tissues were sectioned with a HM325 microtome (Thermo-Fisher Scientific, 902100A) at 8–12 μm thickness. Slides were baked for 1 hour at 55°C. Baked slides were H&E stained following standard procedures. For IHC, sections were deparaffinized, boiled in antigen-retrieval solution, treated with UCP1 antibody (1:200, Abcam, ab23841), and stained with Vectastain ABC KIT (Vector Laboratories, PK-6100) and DAB kit (Vector Laboratories, SK-4100). For indirect immunofluorescence, samples were pre-incubated with permeabilization buffer (0.3% Triton X-100 in PBS) for 30 min at room temperature and then incubated sequentially with primary antibody (4°C, overnight) and secondary antibody (2 hours at room temperature), all in blocking buffer (5% normal donkey serum in 1X PBS). Antibodies used for immunostaining are: rabbit-anti-UCP1 (1:200, Abcam, ab23841), mouse-anti-RFP (1:200, Clontech, 632392), chicken-anti-GFP (1:500, Abcam, ab13970), goat-anti-Perilipin (1:500, Abcam, ab61682). Secondary antibodies including Alexa Fluor® 488 donkey anti-rabbit (711–545-152), Alexa Fluor® 488 donkey anti-chicken (703–545-155), cy3 donkey anti-mouse (715–165-150) and Cy™5 donkey anti-goat (705–175-147) were from Jackson ImmunoResearch. All secondary antibodies were used at a 1:500 dilution. To stain lipid, chopped adipose tissue were incubated in LipidTox Deep Red (Invitrogen, H34477) at 1:200 in PBS for overnight at 4°C before washing in PBS and mounting for imaging. Immunostaining images were collected on a Zeiss LSM500 confocal microscope or a Leica DMi8 inverted microscope. Whole-mount images were taken on a Leica M205FA fully motorized stereo microscope. For quantification of images, two independent observers assessed 3 random fields in 10 random sections from at least 3 mice per cohort and used ImageJ (NIH).

## Oil Red O staining

*In vitro* differentiated cells were fixed with 4% paraformaldehyde for 45 minutes at room temperature. After washing the cells with tap water twice, they were incubated in 60% isopropanol for 10 minutes. The cells were then stained with Oil Red O working solution (Sigma-Aldrich, O1391, 0.5% isopropanol) at room temperature for 30 minutes. After removing the Oil Red O solution, the cells were washed with running tap water, and images were acquired for analysis.

### Metabolic Phenotyping Experiments

Fat content was analyzed using a Bruker minispec whole body composition analyzer. For glucose monitoring, tail blood was drawn in the morning (9am CST), and blood glucose levels were measured using a Contour glucometer (Bayer). Glucose and insulin tolerance tests were performed by injecting 1.25 mg glucose or 1.5mU Humalog (Lilly)/g mouse weight intraperitoneally (IP) after a 5-hour fast, and blood glucose levels were measured at the indicated intervals.

### Body temperature and cold exposure

To conduct cold experiments, mice were exposed to a 6°C cold environmental chamber (Power Scientific, RIS70SD) or kept at room temperature (22°C) for seven days. Rectal temperature was measured daily using a lubricated (100% glycerol) rectal probe (Physitemp, TH-5 Thermalert Monitoring Thermometer), which was inserted 1.27 centimeters (1/2 inch) and the temperature was recorded once it stabilized.

### Statistical Analysis

Statistical significance was assessed by two-tailed Student’s t test or one-way ANOVA followed by post hoc comparisons using the Bonferroni post hoc test. Data were plotted using OriginLab 8.0 or GraphPad Prism 9.0, and a p-value of $< 0.05$ was considered statistically significant. The data are presented as means with error bars indicating ± SEM, and all experiments were conducted with a minimum of 3 mice per group across 2–3 independent cohorts. Male mice were used at the specified ages, and no mice were excluded from the study unless visible fight wounds were observed.

## Supplementary Material

Refer to Web version on PubMed Central for supplementary material.

## ACKNOWLEDGEMENTS

The authors gratefully acknowledge the Department of Internal Medicine and Developmental Biology, as well as the Flow Core Facility at UT Southwestern Medical Center, for their scientific and technical support. We also extend our thanks to Ajin Lim for maintaining mouse husbandry and to the Mouse Metabolic Phenotyping Core at UT Southwestern Medical Center at Dallas. Special thanks to Drs. Cynthia Rose Adams and Jeanette Purcell for their assistance with mouse husbandry, Dr. Stefan J. Green and the Research Resources Center for real-time qPCR analysis at the University of Illinois at Chicago. We are also grateful for the support and advice of Jonathan Graff and for the helpful comments provided by members of the Jiang laboratory on the manuscript. This work was supported by the National Institute of Diabetes and Digestive and Kidney Disease grant K01 DK111771, R03 DK127149 and R01 DK132398 to Y.J., China Postdoctoral Science Foundation (2021M701264) and GuangDong Basic and Applied Basic Research Foundation (2022A1515111158) to Y.Y., R01 grant HL148756 to O.S, and R01 grant NIAAA R01AA026603 to Z.S.

## REFERENCES

Angueira AR, Sakers AP, Holman CD, Cheng L, Arbocco MN, Shamsi F, Lynes MD, Shrestha R, Okada C, Batmanov K, et al. (2021). Defining the lineage of thermogenic perivascular adipose tissue. Nat Metab 3, 469–484. 10.1038/s42255-021-00380-0. [PubMed: 33846639]

Belfiore A, Frasca F, Pandini G, Sciacca L, and Vigneri R (2009). Insulin receptor isoforms and insulin receptor/insulin-like growth factor receptor hybrids in physiology and disease. Endocr Rev 30, 586–623. 10.1210/er.2008-0047. [PubMed: 19752219]

Berry DC, Jiang Y, and Graff JM (2016a). Emerging Roles of Adipose Progenitor Cells in Tissue Development, Homeostasis, Expansion and Thermogenesis. Trends Endocrinol Metab 27, 574–585. 10.1016/j.tem.2016.05.001. [PubMed: 27262681]

Berry DC, Jiang Y, and Graff JM (2016b). Mouse strains to study cold-inducible beige progenitors and beige adipocyte formation and function. Nat Commun 7, 10184. 10.1038/ncomms10184. [PubMed: 26729601]

Berry DC, and Noy N (2009). All-trans-retinoic acid represses obesity and insulin resistance by activating both peroxisome proliferation-activated receptor beta/delta and retinoic acid receptor. Mol Cell Biol 29, 3286–3296. 10.1128/MCB.01742-08. [PubMed: 19364826]

Berry DC, Soltanian H, and Noy N (2010). Repression of cellular retinoic acid-binding protein II during adipocyte differentiation. J Biol Chem 285, 15324–15332. M110.110635 [pii] 10.1074/jbc.M110.110635. [PubMed: 20228061]

Bluher M, Kahn BB, and Kahn CR (2003). Extended longevity in mice lacking the insulin receptor in adipose tissue. Science 299, 572–574. 10.1126/science.1078223299/5606/572 [pii]. [PubMed: 12543978]

Bluher M, Michael MD, Peroni OD, Ueki K, Carter N, Kahn BB, and Kahn CR (2002). Adipose tissue selective insulin receptor knockout protects against obesity and obesity-related glucose intolerance. Dev Cell 3, 25–38. 10.1016/s1534-5807(02)00199-5. [PubMed: 12110165]

Boucher J, Kleinridders A, and Kahn CR (2014). Insulin receptor signaling in normal and insulin-resistant states. Cold Spring Harb Perspect Biol 6. 10.1101/cshperspect.a009191.

Boucher J, Softic S, El Ouaamari A, Krumpoch MT, Kleinridders A, Kulkarni RN, O'Neill BT, and Kahn CR (2016). Differential Roles of Insulin and IGF-1 Receptors in Adipose Tissue Development and Function. Diabetes 65, 2201–2213. 10.2337/db16-0212. [PubMed: 27207537]

Bruning JC, Gautam D, Burks DJ, Gillette J, Schubert M, Orban PC, Klein R, Krone W, Muller-Wieland D, and Kahn CR (2000). Role of brain insulin receptor in control of body weight and reproduction. Science 289, 2122–2125. [PubMed: 11000114]

Bruning JC, Michael MD, Winnay JN, Hayashi T, Horsch D, Accili D, Goodyear LJ, and Kahn CR (1998). A muscle-specific insulin receptor knockout exhibits features of the metabolic syndrome of NIDDM without altering glucose tolerance. Mol Cell 2, 559–569. S1097–2765(00)80155–0 [pii]. [PubMed: 9844629]

Choowong-In P, Sattayasai J, Poodendaen C, and Iamsaard S (2021). Decreased expression of AKAP4 and TyrPho proteins in testis, epididymis, and spermatozoa with low sexual performance of mice induced by modified CUMS. Andrologia 53, e13977. 10.1111/and.13977. [PubMed: 33486757]

Coutinho T, Goel K, Correa de Sa D, Kragelund C, Kanaya AM, Zeller M, Park JS, Kober L, Torp-Pedersen C, Cottin Y, et al. (2011). Central obesity and survival in subjects with coronary artery disease: a systematic review of the literature and collaborative analysis with individual subject data. J Am Coll Cardiol 57, 1877–1886. 10.1016/j.jacc.2010.11.058. [PubMed: 21545944]

Czech MP (2017). Insulin action and resistance in obesity and type 2 diabetes. Nat Med 23, 804–814. 10.1038/nm.4350. [PubMed: 28697184]

Emerging Risk Factors C, Wormser D, Kaptoge S, Di Angelantonio E, Wood AM, Pennells L, Thompson A, Sarwar N, Kizer JR, Lawlor DA, et al. (2011). Separate and combined associations of body-mass index and abdominal adiposity with cardiovascular disease: collaborative analysis of 58 prospective studies. Lancet 377, 1085–1095. 10.1016/S0140-6736(11)60105-0. [PubMed: 21397319]

Horsley V, and Watt F (2017). Repeal and Replace: Adipocyte Regeneration in Wound Repair. Cell Stem Cell 20, 424–426. 10.1016/j.stem.2017.03.015. [PubMed: 28388424]

Jeffery E, Church CD, Holtrup B, Colman L, and Rodeheffer MS (2015). Rapid depot-specific activation of adipocyte precursor cells at the onset of obesity. Nat Cell Biol 17, 376–385. 10.1038/ncb3122. [PubMed: 25730471]

Jiang Y, Berry DC, and Graff J (2017a). Distinct cellular and molecular mechanisms for beta3 adrenergic receptor induced beige adipocyte formation. Elife 6. 10.7554/eLife.30329.

Jiang Y, Berry DC, Jo A, Tang W, Arpke RW, Kyba M, and Graff JM (2017b). A PPARgamma transcriptional cascade directs adipose progenitor cell-niche interaction and niche expansion. Nat Commun 8, 15926. 10.1038/ncomms15926. [PubMed: 28649987]

Jiang Y, Berry DC, Tang W, and Graff JM (2014). Independent stem cell lineages regulate adipose organogenesis and adipose homeostasis. Cell Rep 9, 1007–1022. 10.1016/j.celrep.2014.09.049. [PubMed: 25437556]

Joshi RL, Lamothe B, Cordonnier N, Mesbah K, Monthioux E, Jami J, and Bucchini D (1996). Targeted disruption of the insulin receptor gene in the mouse results in neonatal lethality. EMBO J 15, 1542–1547. [PubMed: 8612577]

Katic M, Kennedy AR, Leykin I, Norris A, McGettrick A, Gesta S, Russell SJ, Bluher M, Maratos-Flier E, and Kahn CR (2007). Mitochondrial gene expression and increased oxidative metabolism: role in increased lifespan of fat-specific insulin receptor knock-out mice. Aging Cell 6, 827–839. ACE346 [pii]10.1111/j.1474-9726.2007.00346.x. [PubMed: 18001293]

Kershaw EE, and Flier JS (2004). Adipose tissue as an endocrine organ. J Clin Endocrinol Metab 89, 2548–2556. 10.1210/jc.2004-0395. [PubMed: 15181022]

Kitamura T, Kahn CR, and Accili D (2003). Insulin receptor knockout mice. Annu Rev Physiol 65, 313–332. 10.1146/annurev.physiol.65.092101.142540092101.142540 [pii]. [PubMed: 12471165]

Knittle JL, Timmers K, Ginsberg-Fellner F, Brown RE, and Katz DP (1979). The growth of adipose tissue in children and adolescents. Cross-sectional and longitudinal studies of adipose cell number and size. J Clin Invest 63, 239–246. 10.1172/JCI109295. [PubMed: 429551]

Kulkarni RN, Bruning JC, Winnay JN, Postic C, Magnuson MA, and Kahn CR (1999). Tissue-specific knockout of the insulin receptor in pancreatic beta cells creates an insulin secretory defect similar to that in type 2 diabetes. Cell 96, 329–339. [PubMed: 10025399]

Long JZ, Svensson KJ, Tsai L, Zeng X, Roh HC, Kong X, Rao RR, Lou J, Lokurkar I, Baur W, et al. (2014). A Smooth Muscle-Like Origin for Beige Adipocytes. Cell Metab. 10.1016/j.cmet.2014.03.025.

Majka SM, Fox KE, Psilas JC, Helm KM, Childs CR, Acosta AS, Janssen RC, Friedman JE, Woessner BT, Shade TR, et al. (2010). De novo generation of white adipocytes from the myeloid lineage via mesenchymal intermediates is age, adipose depot, and gender specific. Proc Natl Acad Sci U S A 107, 14781–14786. 10.1073/pnas.1003512107. [PubMed: 20679227]

Mauer J, Chaurasia B, Plum L, Quast T, Hampel B, Bluher M, Kolanus W, Kahn CR, and Bruning JC (2010). Myeloid cell-restricted insulin receptor deficiency protects against obesity-induced inflammation and systemic insulin resistance. PLoS Genet 6, e1000938. 10.1371/journal.pgen.1000938. [PubMed: 20463885]

Nakae J, Kido Y, and Accili D (2001). Distinct and overlapping functions of insulin and IGF-I receptors. Endocr Rev 22, 818–835. 10.1210/edrv.22.6.0452. [PubMed: 11739335]

Phillips LK, and Prins JB (2008). The link between abdominal obesity and the metabolic syndrome. Curr Hypertens Rep 10, 156–164. 10.1007/s11906-008-0029-7. [PubMed: 18474184]

Pischon T, Boeing H, Hoffmann K, Bergmann M, Schulze MB, Overvad K, van der Schouw YT, Spencer E, Moons KG, Tjonneland A, et al. (2008). General and abdominal adiposity and risk of death in Europe. N Engl J Med 359, 2105–2120. 10.1056/NEJMoa0801891. [PubMed: 19005195]

Plikus MV, Guerrero-Juarez CF, Ito M, Li YR, Dedhia PH, Zheng Y, Shao M, Gay DL, Ramos R, Hsi TC, et al. (2017). Regeneration of fat cells from myofibroblasts during wound healing. Science 355, 748–752. 10.1126/science.aai8792. [PubMed: 28059714]

Pratipanawatr W, Pratipanawatr T, Cusi K, Berria R, Adams JM, Jenkinson CP, Maezono K, DeFronzo RA, and Mandarino LJ (2001). Skeletal muscle insulin resistance in normoglycemic subjects with a strong family history of type 2 diabetes is associated with decreased insulin-stimulated insulin receptor substrate-1 tyrosine phosphorylation. Diabetes 50, 2572–2578. [PubMed: 11679436]

Qiang G, Whang Kong H, Xu S, Pham HA, Parlee SD, Burr AA, Gil V, Pang J, Hughes A, Gu X, et al. (2016). Lipodystrophy and severe metabolic dysfunction in mice with adipose tissue-specific insulin receptor ablation. Mol Metab 5, 480–490. 10.1016/j.molmet.2016.05.005. [PubMed: 27408774]

Reyne Y, Nougues J, and Vezinhet A (1983). Adipose tissue regeneration in 6-month-old and adult rabbits following lipectomy. Proc Soc Exp Biol Med 174, 258–264. [PubMed: 6634719]

Rosen ED, and Spiegelman BM (2006). Adipocytes as regulators of energy balance and glucose homeostasis. Nature 444, 847–853. nature05483 [pii]10.1038/nature05483. [PubMed: 17167472]

Rosen ED, and Spiegelman BM (2014). What we talk about when we talk about fat. Cell 156, 20–44. 10.1016/j.cell.2013.12.012. [PubMed: 24439368]

Sakaguchi M, Fujisaka S, Cai W, Winnay JN, Konishi M, O'Neill BT, Li M, Garcia-Martin R, Takahashi H, Hu J, et al. (2017). Adipocyte Dynamics and Reversible Metabolic Syndrome in Mice with an Inducible Adipocyte-Specific Deletion of the Insulin Receptor. Cell Metab 25, 448–462. 10.1016/j.cmet.2016.12.008. [PubMed: 28065828]

Shamsi F, Piper M, Ho LL, Huang TL, Gupta A, Streets A, Lynes MD, and Tseng YH (2021). Vascular smooth muscle-derived Trpv1(+) progenitors are a source of cold-induced thermogenic adipocytes. Nat Metab 3, 485–495. 10.1038/s42255-021-00373-z. [PubMed: 33846638]

Shao M, Hepler C, Vishvanath L, MacPherson KA, Busbuso NC, and Gupta RK (2017). Fetal development of subcutaneous white adipose tissue is dependent on Zfp423. Mol Metab 6, 111–124. 10.1016/j.molmet.2016.11.009. [PubMed: 28123942]

Shin S, El-Sabbagh AS, Lukas BE, Tanneberger SJ, and Jiang Y (2020a). Adipose stem cells in obesity: challenges and opportunities. Biosci Rep 40. 10.1042/BSR20194076.

Shin S, Pang Y, Park J, Liu L, Lukas BE, Kim SH, Kim KW, Xu P, Berry DC, and Jiang Y (2020b). Dynamic control of adipose tissue development and adult tissue homeostasis by platelet-derived growth factor receptor alpha. Elife 9. 10.7554/eLife.56189.

Spalding KL, Arner E, Westermark PO, Bernard S, Buchholz BA, Bergmann O, Blomqvist L, Hoffstedt J, Naslund E, Britton T, et al. (2008). Dynamics of fat cell turnover in humans. Nature 453, 783–787. nature06902 [pii]10.1038/nature06902. [PubMed: 18454136]

Spiegelman BM, and Flier JS (2001). Obesity and the regulation of energy balance. Cell 104, 531–543. S0092–8674(01)00240–9 [pii]. [PubMed: 11239410]

Sun K, Kusminski CM, and Scherer PE (2011). Adipose tissue remodeling and obesity. J Clin Invest 121, 2094–2101. 10.1172/JCI45887. [PubMed: 21633177]

Tang W, Zeve D, Seo J, Jo AY, and Graff JM (2011). Thiazolidinediones regulate adipose lineage dynamics. Cell Metab 14, 116–122. S1550–4131(11)00218-X [pii]10.1016/j.cmet.2011.05.012. [PubMed: 21723509]

Tang W, Zeve D, Suh JM, Bosnakovski D, Kyba M, Hammer RE, Tallquist MD, and Graff JM (2008). White fat progenitor cells reside in the adipose vasculature. Science 322, 583–586. 1156232 [pii]10.1126/science.1156232. [PubMed: 18801968]

Taniguchi CM, Emanuelli B, and Kahn CR (2006). Critical nodes in signalling pathways: insights into insulin action. Nat Rev Mol Cell Biol 7, 85–96. nrm1837 [pii]10.1038/nrm1837. [PubMed: 16493415]

Traktuev DO, Merfeld-Clauss S, Li J, Kolonin M, Arap W, Pasqualini R, Johnstone BH, and March KL (2008). A population of multipotent CD34-positive adipose stromal cells share pericyte and mesenchymal surface markers, reside in a periendothelial location, and stabilize endothelial networks. Circ Res 102, 77–85. CIRCRESAHA.107.159475 [pii]10.1161/CIRCRESAHA.107.159475. [PubMed: 17967785]

Trayhurn P, and Beattie JH (2001). Physiological role of adipose tissue: white adipose tissue as an endocrine and secretory organ. Proc Nutr Soc 60, 329–339. 10.1079/pns200194. [PubMed: 11681807]

Vishvanath L, MacPherson KA, Hepler C, Wang QA, Shao M, Spurgin SB, Wang MY, Kusminski CM, Morley TS, and Gupta RK (2016). Pdgfrbeta(+) Mural Preadipocytes Contribute to Adipocyte Hyperplasia Induced by High-Fat-Diet Feeding and Prolonged Cold Exposure in Adult Mice. Cell Metab 23, 350–359. 10.1016/j.cmet.2015.10.018. [PubMed: 26626462]

Wang QA, Tao C, Gupta RK, and Scherer PE (2013). Tracking adipogenesis during white adipose tissue development, expansion and regeneration. Nat Med 19, 1338–1344. 10.1038/nm.3324 nm.3324 [pii]. [PubMed: 23995282]

Wang QA, Tao C, Jiang L, Shao M, Ye R, Zhu Y, Gordillo R, Ali A, Lian Y, Holland WL, et al. (2015). Distinct regulatory mechanisms governing embryonic versus adult adipocyte maturation. Nat Cell Biol 17, 1099–1111. 10.1038/ncb3217. [PubMed: 26280538]

Wu J, Bostrom P, Sparks LM, Ye L, Choi JH, Giang AH, Khandekar M, Virtanen KA, Nuutila P, Schaart G, et al. (2012). Beige adipocytes are a distinct type of thermogenic fat cell in mouse and

human. Cell 150, 366–376. S0092–8674(12)00595–8 [pii]10.1016/j.cell.2012.05.016. [PubMed: 22796012]

Zeve D, Millay DP, Seo J, and Graff JM (2016). Exercise-Induced Skeletal Muscle Adaptations Alter the Activity of Adipose Progenitor Cells. PLoS One 11, e0152129. 10.1371/journal.pone.0152129. [PubMed: 27015423]

Zeve D, Seo J, Suh JM, Stenesen D, Tang W, Berglund ED, Wan Y, Williams LJ, Lim A, Martinez MJ, et al. (2012). Wnt signaling activation in adipose progenitors promotes insulin-independent muscle glucose uptake. Cell Metab 15, 492–504. 10.1016/j.cmet.2012.03.010S1550-4131(12)00106-4 [pii]. [PubMed: 22482731]

Zhang Q, Shan B, Guo L, Shao M, Vishvanath L, Elmquist G, Xu L, and Gupta RK (2022). Distinct functional properties of murine perinatal and adult adipose progenitor subpopulations. Nat Metab 4, 1055–1070. 10.1038/s42255-022-00613-w. [PubMed: 35982290]

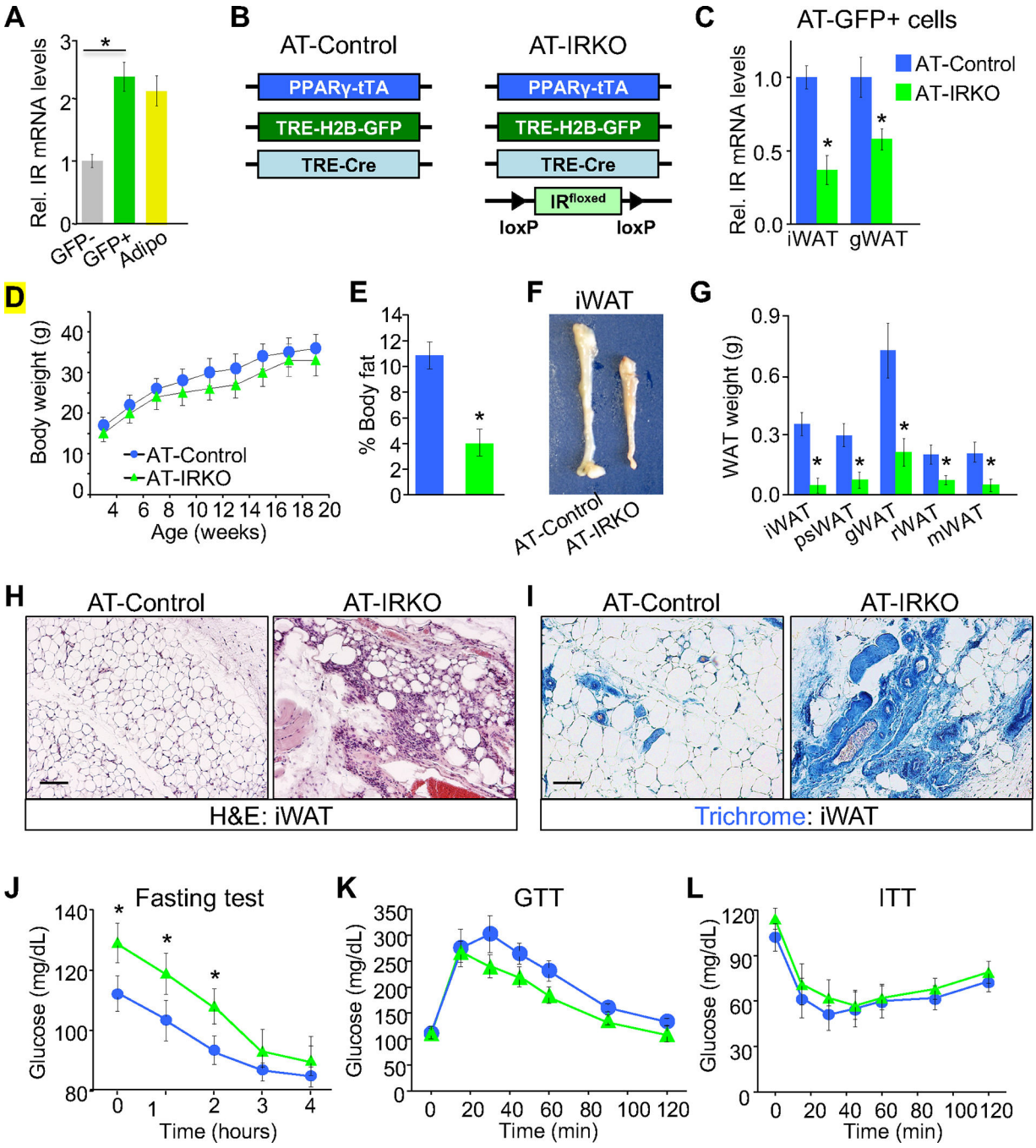


**Figure 1. Deleting IR within Pparγ+ APCs promotes lipodystrophy.**

(A) mRNA levels of IR within different adipose tissue compartments (AT-GFP+, AT-GFP−, and adipocytes) from male mice at P60. Data is presented as the Mean ± SEM n=6 *p<0.05 by T-test.

(B) Illustration of genetic alleles used to create AT-Control and AT-IRKO mice (*Pparγ-tTA/+; TRE-Cre; TRE-H2B-GFP; IR$^{fl/fl}$*); mice were analyzed at P60.

(C) mRNA levels of IR within AT-GFP+ cells of iWAT and gWAT isolated from AT-Control and AT-IRKO mice at P60.

(D) Body weight chase of AT-Control and AT-IRKO mice at P60.
(E) Body fat of AT-Control and AT-IRKO mice from mice described in (B).
(F) Representative pictures of iWAT of AT-Control and AT-IRKO mice.
(G) Adipose depot weights of AT-Control and AT-IRKO mice described in (B).
(H) Representative images of H&E staining of iWAT sections from AT-Control and AT-IRKO mice described in (B).
(I) Representative images of trichrome staining of iWAT sections from AT-Control and AT-IRKO mice described in (B).
(J-L) Fasting (J), GTT (K), ITT (L) glucose levels of AT-Control and AT-IRKO mice described in (B). For (C-L) data is presented as the Mean ± SEM, n=4–6, *P ≤ 0.05 by T-test mutant compared to control levels. Magnification 20X. Scale bar=100 μm.

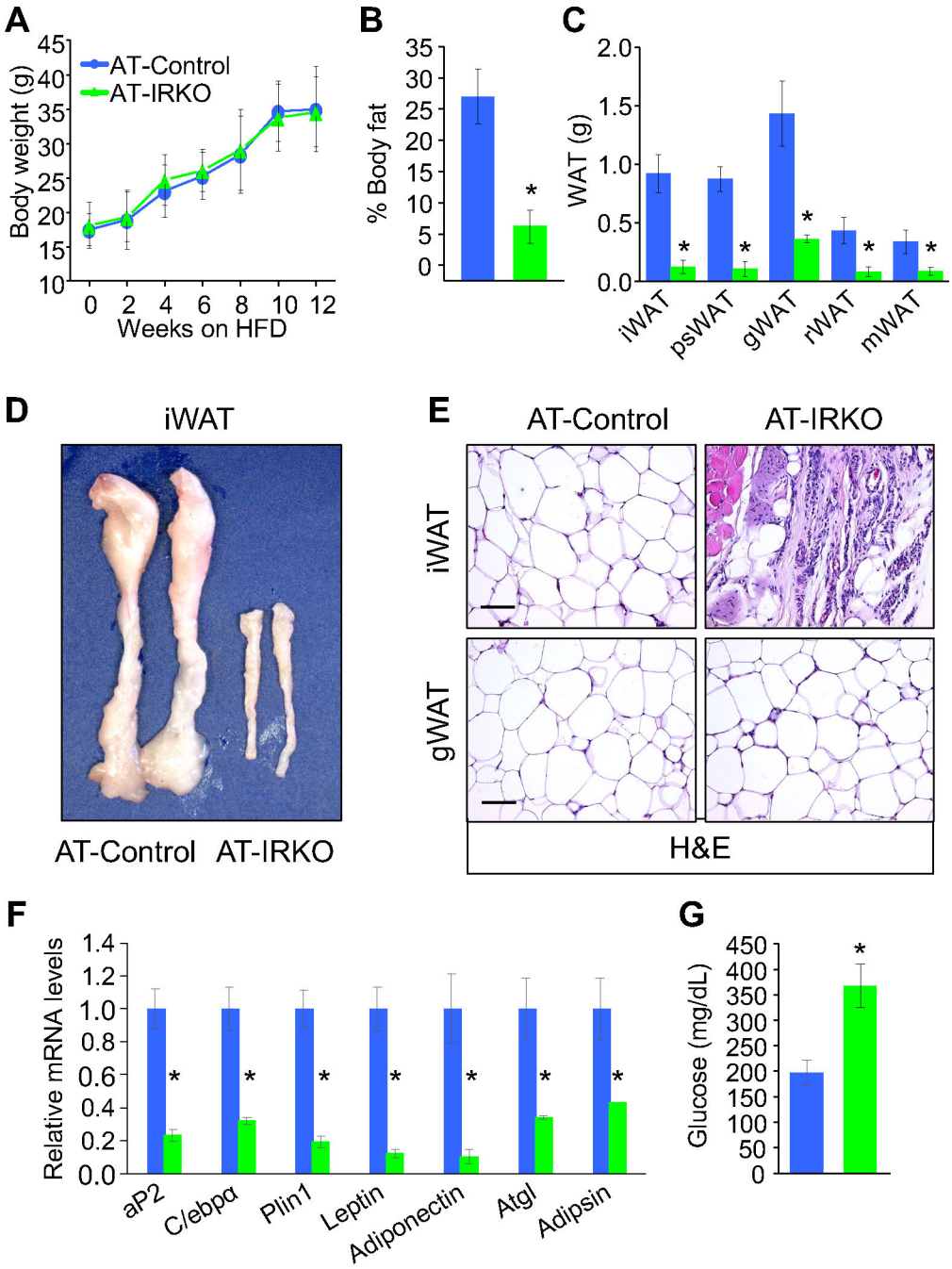


**Figure 2. HFD does not restore fat formation in AT-IRKO mice.**

Two-month-old AT-Control and AT-IRKO male mice were fed a HFD for 12 weeks.

(A) Body weight curve throughout the HFD period.

(B, C) Percent body fat (B) and adipose tissue weight (C) from AT-Control and AT-IRKO post-HFD.

(D) Representative pictures of iWAT of AT-Control and AT-IRKO post-HFD.

(E) Representative images of H&E staining of iWAT and gWAT sections from AT-Control and AT-IRKO post-HFD.

(F) mRNA levels of white adipocyte gene markers from iWAT depots from AT-Control and AT-IRKO post-HFD.
(G) Random fed serum glucose levels of AT-Control and AT-IRKO post-HFD. Data is presented as the Mean ± SEM, n=4–6, *P ≤ 0.05 by T-test mutant compared to control levels. Magnification 20X. Scale bar=100 μm.

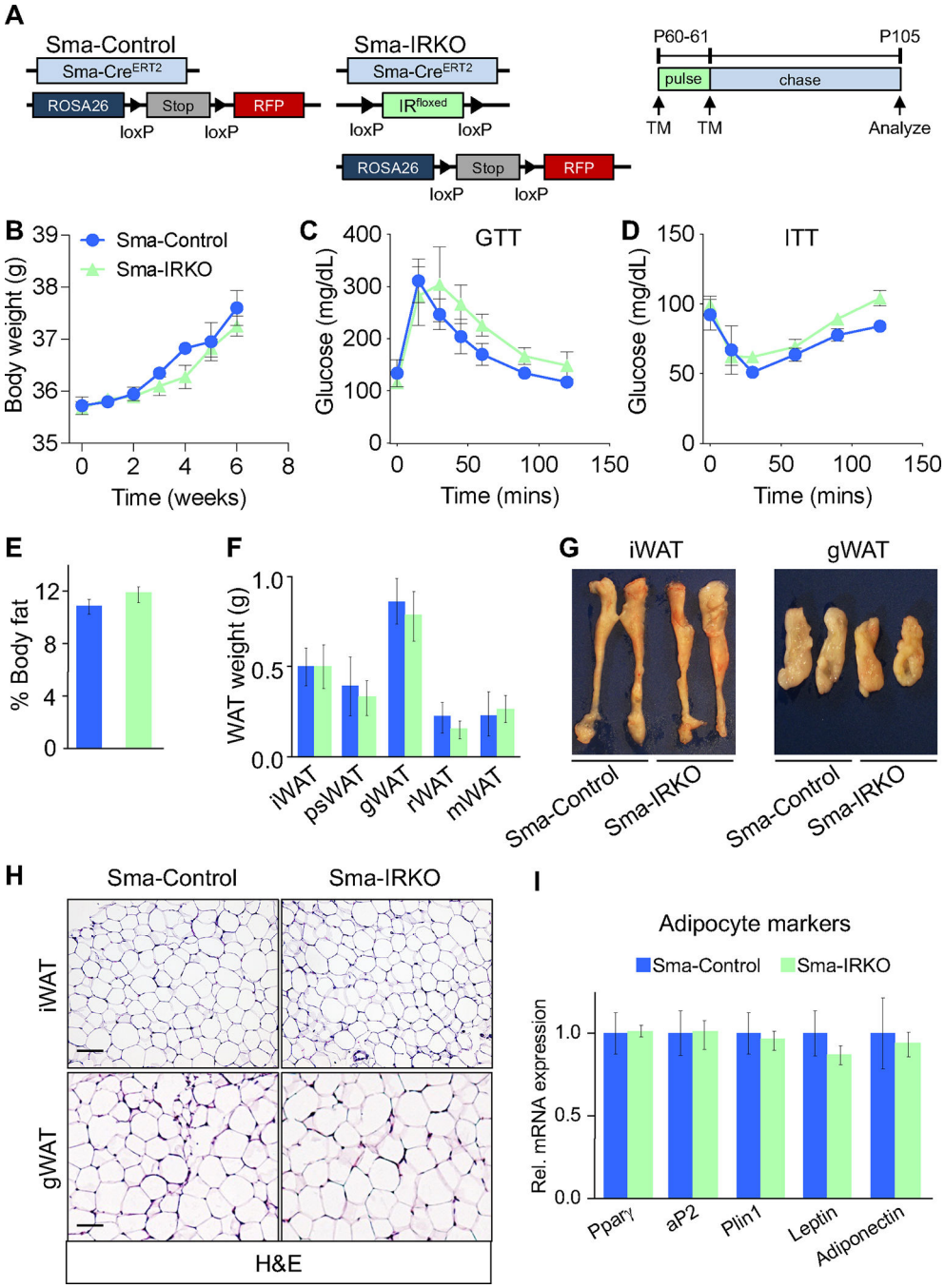


**Figure 3. Deleting IR within adult Sma+ APCs does not impact WAT homeostasis.**

(A) Experimental paradigm: Two-month-old *Sma-Cre$^{ERT2}$; R26R$^{RFP}$* mice (Sma-Control) and *Sma-Cre$^{ERT2}$; IR$^{fl/fl}$; R26R$^{RFP}$* (Sma-IRKO) mice were administered one dose of tamoxifen (50 mg/Kg) for two consecutive days (n=5) and mice were phenotypically assessed six-weeks later.

(B) Body weight curve of Sma-Control and Sma-IRKO mice throughout the experimental period.

(C, D) GTT (C) or ITT (D) of Sma-Control and Sma-IRKO mice described in (A).

(E) Percent body fat (E) and WAT weight (F) of Sma-Control and Sma-IRKO mice described in (A).
(G) Representative pictures of iWAT and gWAT from Sma-Control and Sma-IRKO mice described in (A).
(H) Representative images of H&E staining of iWAT and gWAT sections from Sma-Control and Sma-IRKO mice described in (A).
(I) mRNA levels of white adipocyte gene markers from iWAT depots from HFD fed Sma-Control and Sma-IRKO mice. Data is presented as the Mean ± SEM, n=5, Magnification 20X. Scale bar=100 μm.

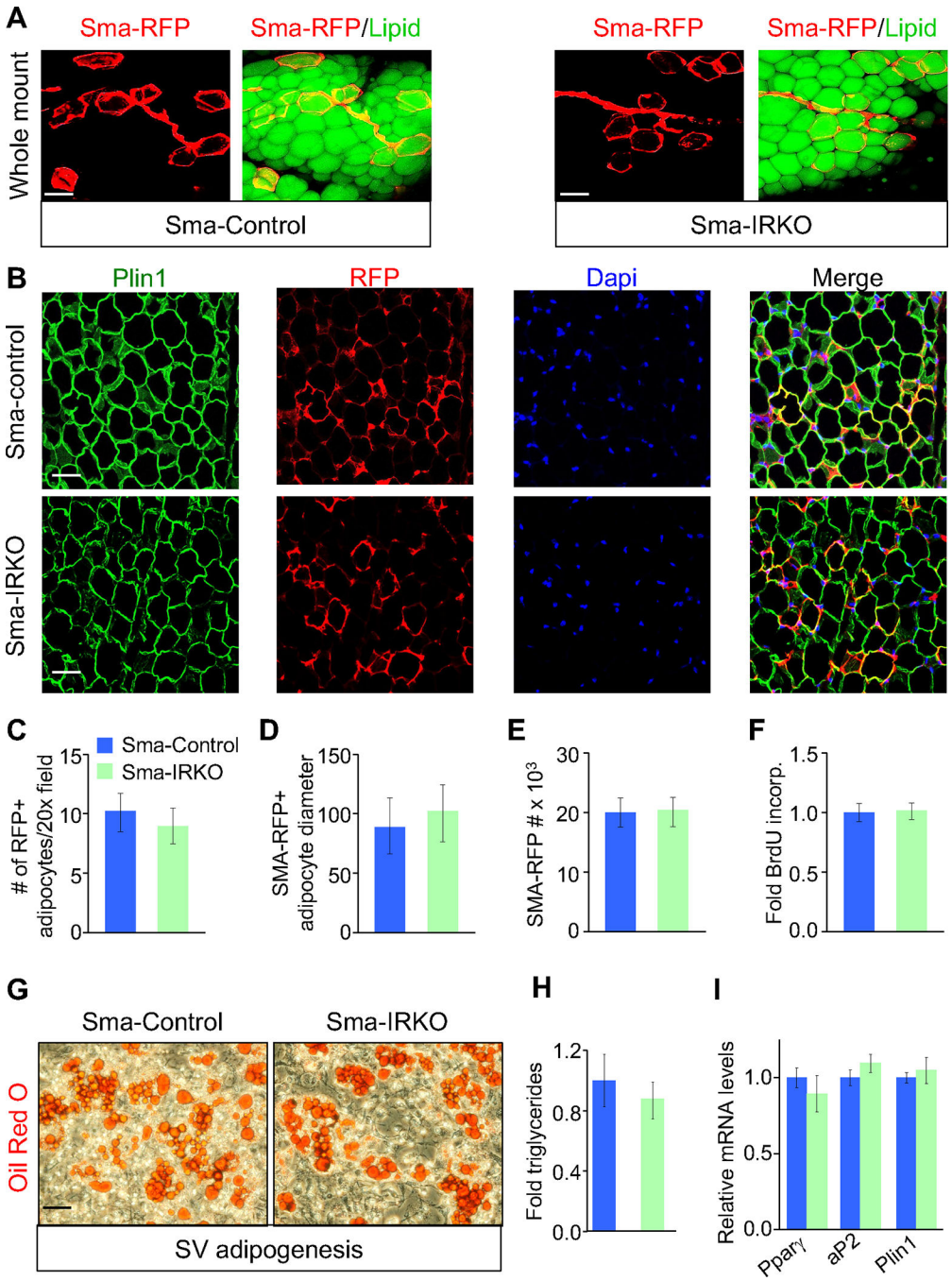


**Figure 4. Deleting IR within adult Sma+ APCs does not impact white adipogenesis.**

(A) Two-month-old Sma-Control and Sma-IRKO mice were administered one dose of TMX for two consecutive days. Mice were evaluated six-weeks post-TMX. Whole mount imaging of Sma-Control and Sma-IRKO iWAT depots stained for LipidTox (green) and visualized for RFP (red) fate mapping analysis.

(B) Representative images of RFP (Sma-driven) fate mapping analysis and Plin1 immunostaining of iWAT sections from Sma-Control and Sma-IRKO mice described in (A).

(C) Quantification of RFP+ adipocytes within iWAT sections from Sma-Control and Sma-IRKO mice described in (A).
(D) Quantification of RFP+ adipocyte diameter from Sma-Control and Sma-IRKO mice described in (A).
(E) Flow cytometric analysis of RFP+ cell number from iWAT SVF from Sma-Control and Sma-IRKO mice.
(F) Flow cytometric analysis of BrdU incorporation into RFP+ cells from iWAT depots from Sma-control and Sma-IRKO mice.
(Choowong-In et al.) SV cells were isolated from iWAT depots from Sma-Control and Sma-IRKO and were induced with white adipogenic media. White adipocyte differentiation was assessed by Oil Red O staining (G), triglyceride accumulation (H), and directed qPCR against adipocyte marker genes (I). Data is presented as the Mean ± SEM, n=5, Magnification 20X. Scale bar=100 μm.

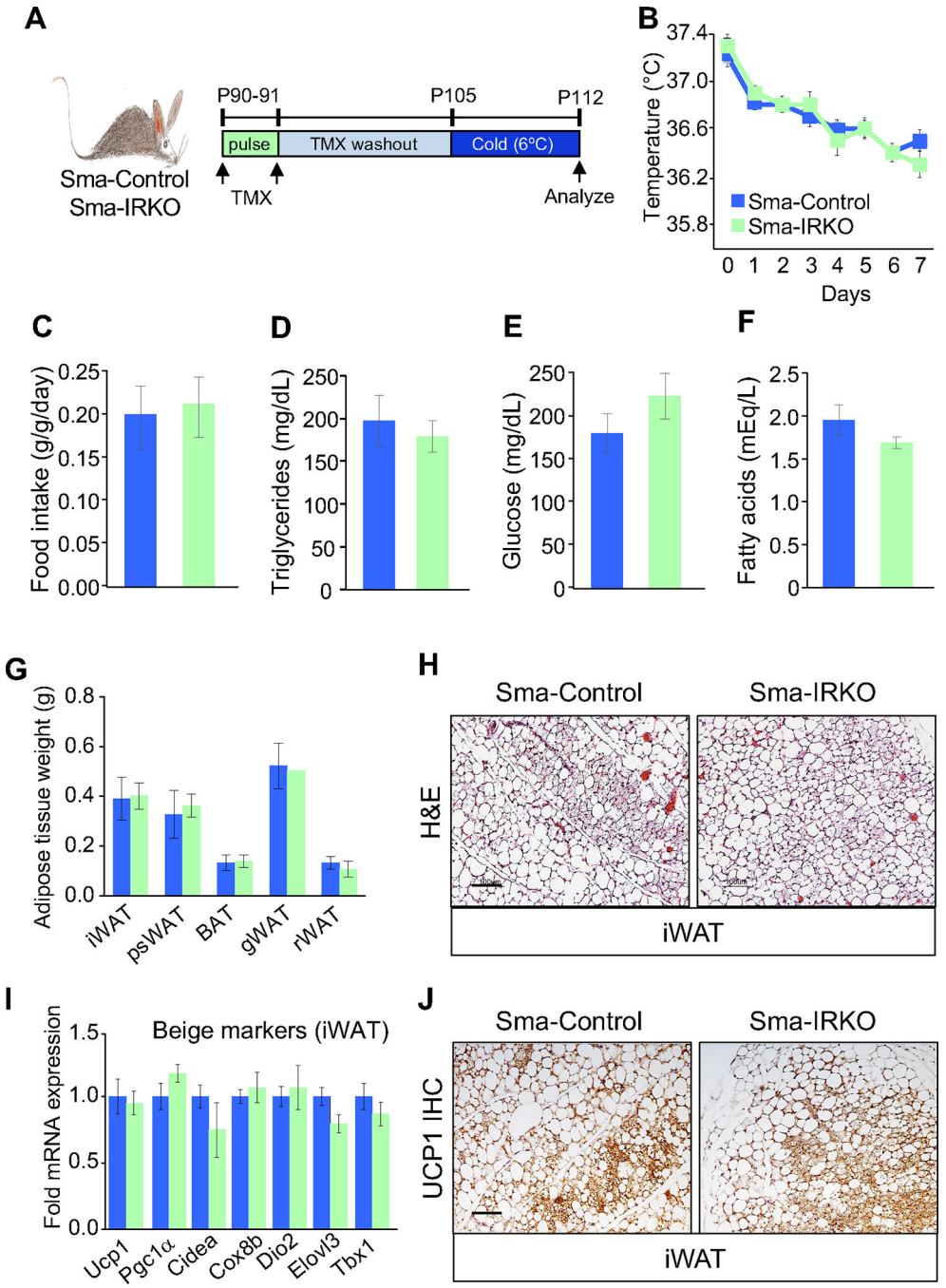


**Figure 5. IR loss in adult Sma+ APCs does not impact cold-induced beige adipogenesis.**

(A) Experimental schema: three-month-old Sma-Control and Sma-IRKO male mice were administered one dose of TMX for two consecutive days and a two-week TMX washout period was observed prior to seven days of cold temperature (6°C) exposure.

(B-F) Rectal temperatures (B), food intake (C), and serum triglycerides (D), glucose (E), and fatty acids (F) were assessed from cold exposed mice described in (A).

(G) Adipose tissue weights from Sma-Control and Sma-IRKO cold exposed mice described in (A).

(H) H&E staining of iWAT sections from cold exposed mice described in (A).
(I) mRNA levels of beige adipocyte gene expression within iWAT depots from cold exposed mice described in (A).
(J) Ucp1 immunohistochemical staining of iWAT sections from cold exposed mice described in (A). Data is presented as the Mean ± SEM, n=4–6, Magnification 20X. Scale bar=100 μm.

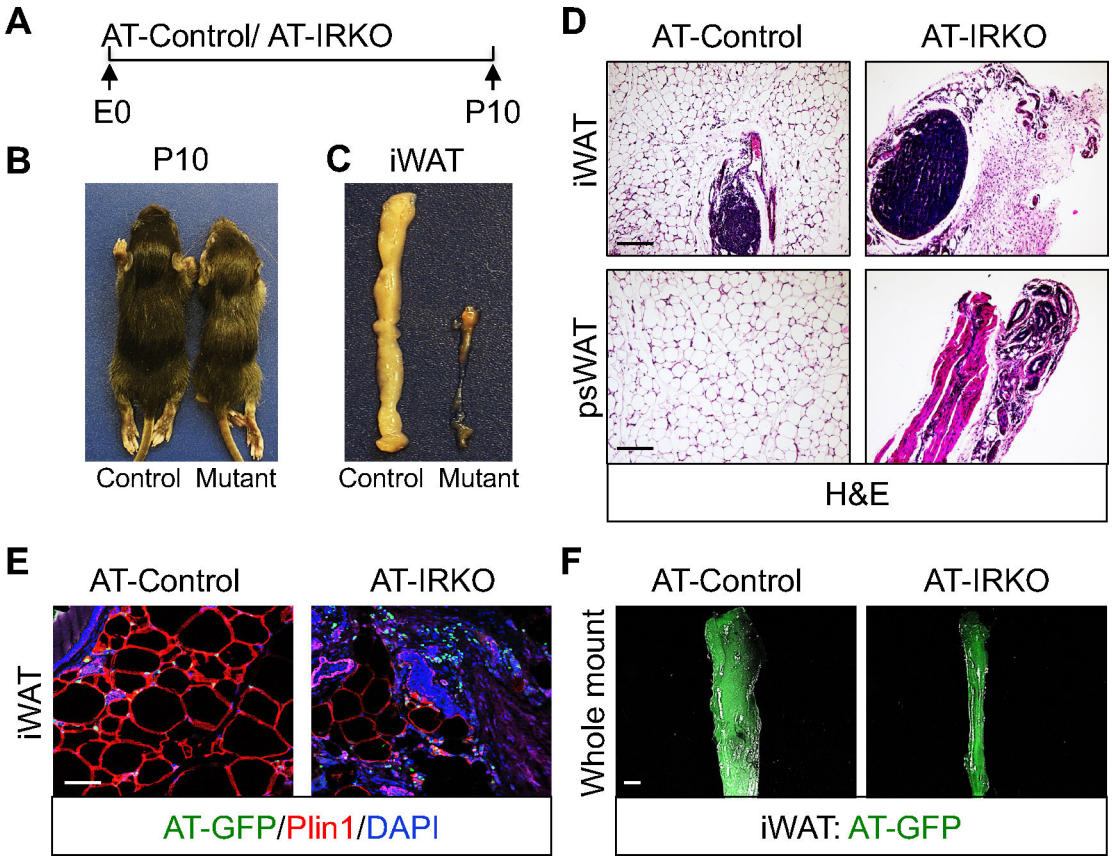


**Figure 6. IR within Pparγ+ APCs is required for WAT organogenesis.**

(A) Experimental paradigm for evaluating AT-Control and AT-IRKO mice at postnatal day P10.

(B) Representative whole-body images of AT-Control and AT-IRKO mice described in (A).

(C) Representative images of iWAT depots from AT-Control and AT-IRKO mice described in (A).

(D) Representative H&E staining of iWAT and psWAT sections from AT-Control and AT-IRKO mice described in (A).

(E) Immunostaining of iWAT sections for GFP (green) and Perilipin-1 (red) from AT-Control and AT-IRKO mice described in (A).

(F) Whole mount GFP images of iWAT from AT-Control and AT-IRKO mice described in (A). n=3–4, Magnification 20X. Scale bar=100 μm.

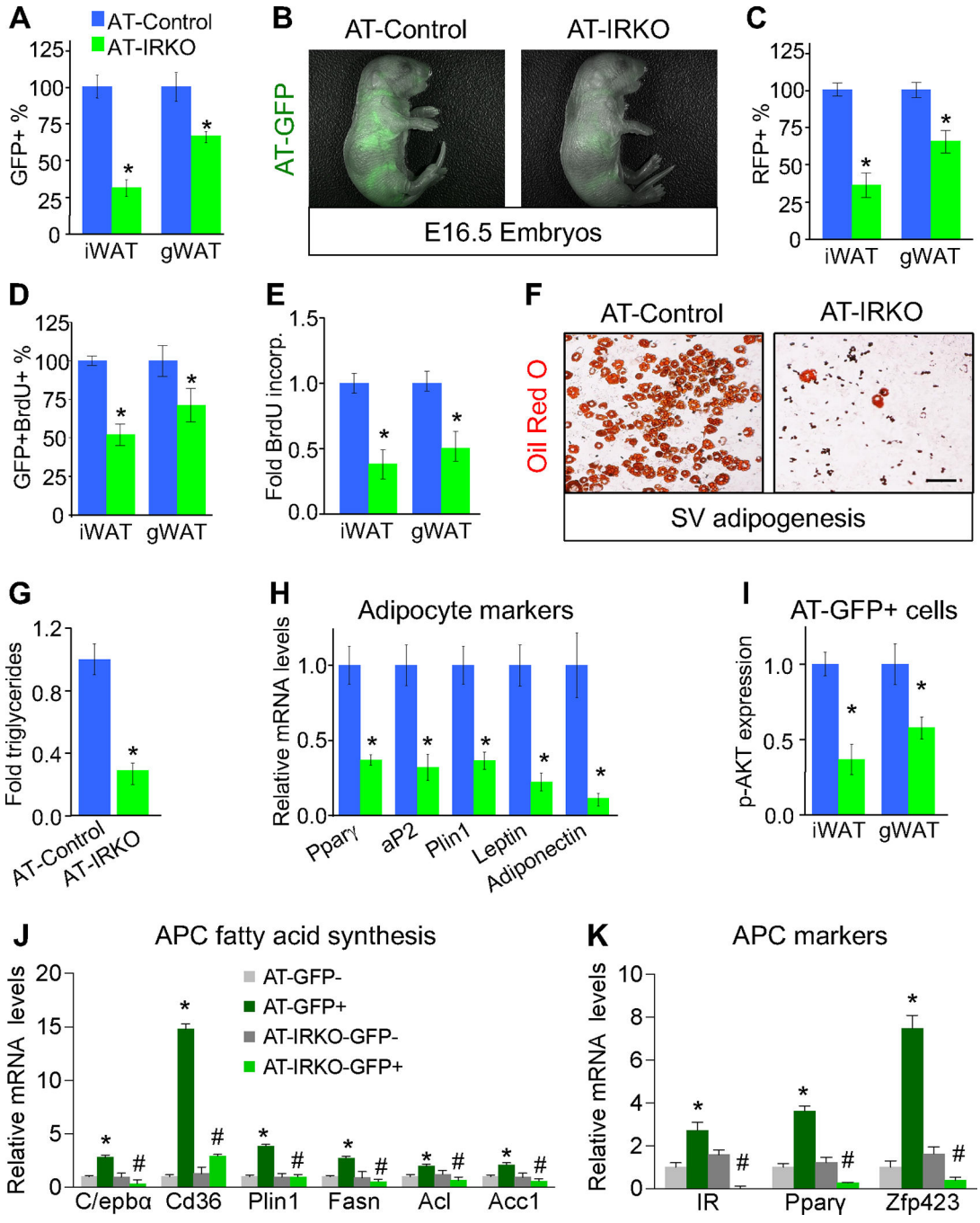


**Figure 7. IR regulates PPARγ+ APC proliferation and genes involved in lipid biogenesis and "stemness".**

(A) Flow cytometric analysis of AT-GFP cell number from iWAT and evolving gWAT depots from P10 AT-Control and AT-IRKO mice.

(B) Representative whole mount images of P10 AT-Control and AT-IRKO E16.5 embryos showing reduced GFP intensity but correct anatomical anlagen.

(C) Flow cytometry analysis of AT-RFP cell number from iWAT and evolving gWAT depots from P10 AT-Control and AT-IRKO mice.

(D) Flow cytometric analysis of AT-GFP-BrdU+ APCs from iWAT and evolving gWAT depots from P10 AT-Control and AT-IRKO mice at P10.
(E) In vitro BrdU incorporation assay performed on AT-GFP+ cells FACS isolated from AT-Control and AT-IRKO mice.
(F-H) SV cells were isolated from iWAT depots from Sma-Control and Sma-IRKO and were induced white adipogenic media. White adipocyte differentiation was assessed by Oil Red O staining (F), triglyceride accumulation (G), and mRNA expression of adipocyte marker genes (H). Magnification 20X. Scale bar=100 μm.
(I) AT-GFP+ cells from P10 AT-Control and AT-IRKO mice were FACS isolated and examined for phosphorylated Akt.
(J) Relative mRNA levels of APC common fatty acid synthesis genes in GFP+ and GFP− cells from control and AT-IRKO mice.
(K) Relative mRNA levels of APC markers in GFP+ and GFP− cells from control and AT-IRKO mice. Data is presented as the Mean ± SEM, n=4–6, $*^{\#}P \leq 0.05$ by T-test mutant compared to control levels.